

# Microsatellite instability induced mutations in DNA repair genes CtIP and MRE11 confer hypersensitivity to poly (ADP-ribose) polymerase inhibitors in myeloid malignancies

Terry J. Gaymes,<sup>1</sup> Azim M. Mohamedali,<sup>1</sup> Miranda Patterson,<sup>2</sup> Nazia Matto,<sup>1</sup> Alexander Smith,<sup>1</sup> Austin Kulasekararaj,<sup>1</sup> Rajani Chelliah,<sup>1</sup> Nicola Curtin,<sup>2</sup> Farzin Farzaneh,<sup>1</sup> Sydney Shall,<sup>1</sup> and Ghulam J. Mufti<sup>1</sup>

<sup>1</sup>Department of Haematological Medicine, King's College London, Leukaemia Sciences Laboratories, The Rayne Institute, Denmark Hill Campus, London UK; and <sup>2</sup>Newcastle University, Northern Institute for Cancer Research, Medical School, Newcastle upon Tyne, UK

## ABSTRACT

Inactivation of the DNA mismatch repair pathway manifests as microsatellite instability, an accumulation of mutations that drives carcinogenesis. Here, we determined whether microsatellite instability in acute myeloid leukemia and myelodysplastic syndrome correlated with chromosomal instability and poly (ADP-ribose) polymerase (PARP) inhibitor sensitivity through disruption of DNA repair function. Acute myeloid leukemia cell lines (n=12) and primary cell samples (n=18), and bone marrow mononuclear cells from high-risk myelodysplastic syndrome patients (n=63) were profiled for microsatellite instability using fluorescent fragment polymerase chain reaction. PARP inhibitor sensitivity was performed using cell survival, annexin V staining and cell cycle analysis. Homologous recombination was studied using immunocytochemical analysis. SNP karyotyping was used to study chromosomal instability. RNA silencing, Western blotting and gene expression analysis was used to study the functional consequences of mutations. Acute myeloid leukemia cell lines (4 of 12, 33%) and primary samples (2 of 18, 11%) exhibited microsatellite instability with mono-allelic mutations in *CtIP* and *MRE11*. These changes were associated with reduced expression of mismatch repair pathway components, MSH2, MSH6 and MLH1. Both microsatellite instability positive primary acute myeloid leukemia samples and cell lines demonstrated a downregulation of homologous recombination DNA repair conferring marked sensitivity to PARP inhibitors. Similarly, bone marrow mononuclear cells from 11 of 56 (20%) patients with *de novo* high-risk myelodysplastic syndrome exhibited microsatellite instability. Significantly, all 11 patients with microsatellite instability had cytogenetic abnormalities with 4 of them (36%) possessing a mono-allelic microsatellite mutation in *CtIP*. Furthermore, 50% reduction in *CtIP* expression by RNA silencing also down-regulated homologous recombination DNA repair responses conferring PARP inhibitor sensitivity, whilst *CtIP* differentially regulated the expression of homologous recombination modulating RecQ helicases, WRN and BLM. In conclusion, microsatellite instability dependent mutations in DNA repair genes, *CtIP* and *MRE11* are detected in myeloid malignancies conferring hypersensitivity to PARP inhibitors. Microsatellite instability is significantly correlated with chromosomal instability in myeloid malignancies.

## Introduction

The DNA Mismatch repair (MMR) pathway corrects DNA replication errors that escape DNA polymerase proof-reading.<sup>1</sup> Mutations in MMR genes such as MSH2 and MLH1 result in the ubiquitous presence of mutations in microsatellite (and other) repeat sequences within DNA, a phenomenon termed, Microsatellite Instability (MSI). MSI contributes to the 'mutator phenotype' in cancer because MSI increases the base mutation rate allowing cells to evolve, grow and survive, especially in colonic cancers.<sup>2,3</sup> About 15% of sporadic colon cancer is attributable to defects in MMR and the consequent MSI phenotype.

Myelodysplastic syndromes (MDS) and acute myeloid leukemia (AML) (MDS/AML) represent a group of clonal disorders characterized by impaired differentiation and an accumulation of hematopoietic stem cells.<sup>4</sup> MDS/AML are also characterized by gross chromosomal instability manifesting

as deletions, translocations and chromosome gains and losses.<sup>5</sup> Chemotherapeutic agents and  $\gamma$ -irradiation cause significant double-strand breaks (DSB) and lead to therapy-related MDS/AML in which chromosomal instability is almost universally detected.<sup>6</sup> Furthermore, karyotyping by single nucleotide polymorphism arrays (SNPA) shows that loss of heterozygosity (LOH) and acquired uniparental disomy (UPD) are common in MDS/AML. Therefore, it has been suggested that the underlying cause of chromosomal instability in these diseases is a defect in double-strand DNA repair.<sup>7</sup> If a breakdown in DNA repair processes is the basis of chromosomal instability, then the particular factors responsible for giving survival advantages to the leukemia clone are in fact targets for therapy. Independently, we and others have realised that other instances of genetic defects in the pathways of double-strand DNA repair, involving homologous recombination (HR), non-homologous end-joining (NHEJ) and other DNA damage response pathways would render

©2013 Ferrata Storti Foundation. This is an open-access paper. doi:10.3324/haematol.2012.079251

The online version of this article has a Supplementary Appendix.

Manuscript received on October 17, 2012. Manuscript accepted on January 14, 2013.

Correspondence: ghulam.mufti@kcl.ac.uk

tumor cells sensitive to poly (ADP-ribose) polymerase inhibitors (PARPi). We have previously demonstrated that the NHEJ major pathway for the repair of double strand DNA breaks is overactive and associated with extensive joining errors in primary AML cells.<sup>8</sup> Moreover, we showed that at least 15% of primary cell samples from MDS/AML patients and related cell lines are sensitive to PARPi, because of the presence of DNA repair defects in HR repair.<sup>9</sup> As PARPi sensitivity has been recently shown to be dependent on inappropriate NHEJ activity as a response to absent HR, AML patients are potential candidates for PARPi therapy.<sup>10</sup> Single agent anti-tumor responses coupled with a wide therapeutic index observed pre-clinically have been influential in moving PARPi into the clinic. There are currently over 60 clinical trials in progress in which PARPi are being tested in a range of malignancies, including breast and ovarian cancers with HR defects by virtue of BRCA mutations.

However, breast and ovarian cancer apart, cancers with BRCA mutations are relatively uncommon. Thus, to fully exploit the therapeutic potential of PARPi one must look beyond BRCA mutations and identify new biomarkers of PARPi sensitivity. This would include mutations in other genes associated with the cellular response to DSB via HR. Indeed, components of the DSB repair signaling pathway such as MRE11A (hereon referred to as MRE11) and ATR have previously been shown to confer PARPi sensitivity.<sup>11,12</sup> Importantly, mutations in DNA repair genes induced by MSI have been shown to further disrupt genomic stability and affect the response to chemotherapy.<sup>13,14</sup> Consequently, we have investigated the possibility that genetic changes that promote leukemic evolution may provide targets for therapeutic intervention, by testing for MSI-dependent alterations in specific DNA repair genes in AML and MDS.

## Methods

### Drugs

The PARPi PJ34 and EB47 were purchased from Calbiochem, Nottingham, UK. The PARPi, BMN 673 and KU-0058948 were kindly donated by Biomarin Pharmaceutical Inc., Novato, CA, USA, and Astra-Zeneca, Cambridge, UK, respectively.

### Patients

Sixty-three MDS patients with a median age of 67 years (range 36-86 years) were risk classified according to IPSS and followed until May 2010 for survival and disease progression. Diagnosis according to the WHO classification for the 63 patients was: 1 refractory anemia (RA), 7 refractory cytopenia with multi-lineage dysplasia (RCMD), 37 refractory anemia with excess blasts (RAEB), 9 AML evolved from MDS (sAML), 5 therapy-related myeloid neoplasms (tMDS/tAML), and 2 chronic myelomonocytic leukemia (CMML). Most of the patients (n=57, 91%) belonged to intermediate-2 or high risk IPSS category. Cytogenetic category as per IPSS risk group were: 19 good risk (30%) (18 patients had normal cytogenetics and one patient had -Y and del20q), 6 intermediate risk (10%), and 38 poor risk (60%). The poor risk cytogenetic group consisted of 12 patients with isolated monosomy 7 (-7/del 7q), 8 with monosomy 7 with one additional aberration, 16 with monosomy 7 with 2 or more aberrations, and 2 complex (3 or more) without abnormal chromosome 7. The median bone marrow blast percentage was 10% (range 0-56%) determined through May-Grunwald-Giemsa staining and CD34<sup>+</sup> phenotyping. Therapy-related MDS (t-MDS) patients received standard

intensive chemotherapy including cytarabine. World Health Organization classification of FAB type for AML for each patient is: M1 n=1, M2 n=2 (including one t-AML), M4 n=4, M5 n=4, M6 n=1. No FAB and cytogenetic data were available for 6 patients (*Online Supplementary Table S1*). All primary AML patient samples contained between 25-100% AML blasts and were taken at first diagnosis apart from the t-AML patient. Primary material was obtained following written informed consent from patients prior to inclusion in the study in accordance with the Declaration of Helsinki by King's College Hospital Local Research Ethics Committee.

### Estimation of Microsatellite Instability

Microsatellite fluorescent fragment PCR was performed using 6 mononucleotide markers; NR21 (21 thymines (T) in the 5' UTR of SLC7A8), NR22 (22T in the 3' UTR of TPPB5), NR24 (24T in the 3' UTR of ZNF-2), BAT25 (25T in intron 16 of C-kit), BAT26 (26A in intron 5 of MSH2) and MONO27 (27T in intron of MAP4K). All markers were amplified in a single multiplex PCR reaction. For DNA repair genes, microsatellite repeats were analyzed using individual PCR reactions. Primer pair sequences are given in the *Online Supplementary Appendix*. Multiplex PCR reactions contained 1  $\mu$ M of each primer and were conducted as previously described<sup>15</sup> (*Online Supplementary Figure S1*).

### Aberrant splicing variations in MRE11 (315del88) and ATM (497del22)

RNA was extracted from cell lines and primary cells in the presence of TRIzol reagent (Invitrogen, Paisley, UK) and reverse transcribed using the SuperScript<sup>®</sup> VIL0™ cDNA Synthesis Kit (Invitrogen) as per the manufacturer's instructions. PCR reactions contained 100 nM primer, Amplitaq 360 taq polymerase/buffer and 1  $\mu$ l of cDNA. The primer pair for MRE11 exon 5 was: 5'-CCAGGGGTTCTTGGAGAAG-3' and 5'-CCAGCACAACCTAAAATGTC-3'. The primer pair for ATM exon 8 was: 5'-CTCAGCAACAGTGGTTAG-3' and 5'-GATATGATTTAGACCTGAAGAG-3' PCR products were visualized by ethidium bromide staining. The ratio of wild-type to variant splice products (Ratio of Intensity, RI) was determined by comparing the intensity of the stained bands on gel photographs using Adobe Photoshop™.

### Cell survival assays

Primary cells (AML or PBL) cell survival was determined using trypan blue exclusion analysis. Counts were performed daily for a period of 120 h after drug addition. Data points were means of 3 separate assays performed per primary sample. For cell lines, soft agar clonogenic assays were performed. Cells were incubated continuously with or without PARPi for 120 h in culture medium. Cells were then seeded in 2.5% bacto-agar (DIFCO) for colony formation. After more than 12 days, colonies were fixed in methanol, visualized by staining with MTT solution in PBS and counted. The plating efficiencies relative to control for each PARPi concentration were calculated to give cell survival as a percentage of control.

### Immunofluorescence

100 nM PARPi was added to 2 x 10<sup>5</sup> cells/mL log phase cell culture (passaged 24 h previously). Incubation with PARPi was for 24 h. Immunofluorescence studies were performed as described.<sup>8</sup> Anti-rad51 (Santa-Cruz), anti-cyclin A (Santa-Cruz) or anti-phospho- $\gamma$ H2AX-FITC (Millipore) were used in this study. Slides were then visualized using an Olympus AX70 epi-fluorescent microscope, and images were captured using a CCD camera and 'smart capture' software. Two slides were prepared for each experiment.

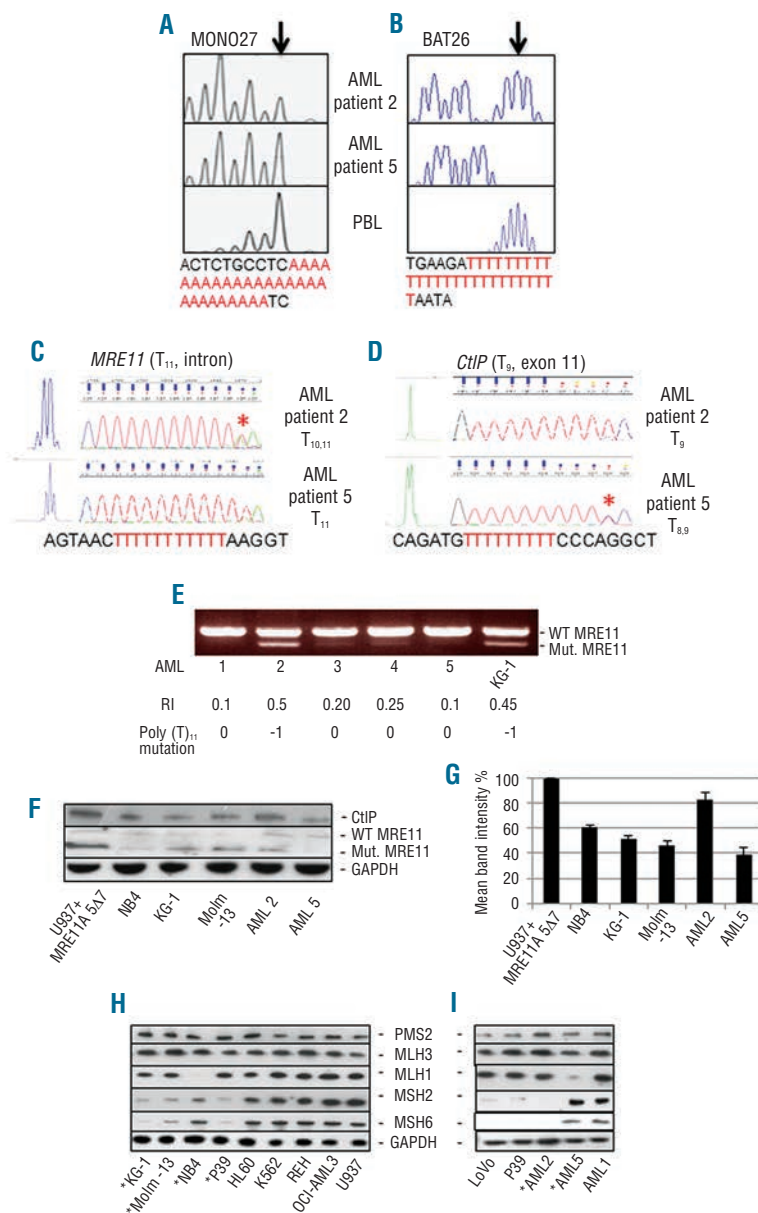


**Figure 1.** Fluorescent fragment PCR and sanger sequencing of DNA repair gene coding region microsatellites. (A-B), MSI loci profiles using fluorescent fragment PCR for MONO27 (A) and BAT26 (B) microsatellites in primary AML cell and normal PBL DNA. Arrows depict mean size of PCR product from normal PBL. Microsatellite sequence is shown under respective profile. (C-D) Fluorescent fragment PCR and sanger sequencing of DNA repair gene coding region microsatellites. DNA from primary AML cells was used in PCR reactions for (C), MRE11, 11 thymine (intronic T<sub>11</sub>), (D), CtIP, 9 thymine microsatellite (T<sub>9</sub>, exon 11). Fluorescent fragment profile is shown in left panel; Sanger sequence is shown in right panel. Asterisks indicate position of deleted nucleotide (E), Aberrant gene transcripts of MRE11 in primary AML. PCR amplification of exon 5 for MRE11 was performed on cDNA from AML patients and KG-1 cells. Ratio of intensities (RI) between wild type (WT) and mutant (mut.) transcript was determined by measuring gel band intensity using Adobe Photoshop™. (F-G) Identification of mutant MRE11 and reduced CtIP expression by Western blotting. (F) Immunoblots were prepared from whole cell extracts of primary AML, MDS/AML cell lines and U937 expressing a mutant MRE11Δ7 construct. Extracts were probed with anti-MRE11 and anti-CtIP. GAPDH acted as a loading control. (G) Graphical quantification of band intensity in Western blots for CtIP expression. Bands Intensity was quantified using Adobe Photoshop™ relative to U937 cells. (H-I) Assessment of MMR expression in MDS/AML primary and cell lines. Immunoblots were prepared from whole cell extracts of primary AML, MDS/AML and colon cancer cell lines and probed with anti-MLH1, anti-MSH2, anti-MLH3, anti-MSH6 or anti-PMS2. GAPDH acted as a loading control. MSI positive cell lines and AML patients are indicated by an asterisk (\*). The immunoblots shown are representative of 6 independent experiments.

Positive cells for phospho- $\gamma$ H2AX and rad51 foci were defined as cells with more than 5 foci after subtracting percentage of cells with more than 5 foci from untreated cells. Percentage of cells with greater than 5 foci in untreated cells ranged from 1-3%. Mean  $\pm$  standard error of the mean (SEM) were determined in 3 separate experiments.

### Transfections

Stable knockdown of MSH2 expression was produced by transfection of Sh-RNA in HUSH expression vectors pGFP-V-RS (Origene, Rockville, MD, USA) into MDS/AML cells. Control vectors without an insert or with a non-effective scrambled Sh-RNA were also transfected into MDS/AML cell lines in separate experiments. Transient knockdown of MSH2 expression in leukemia cells was achieved by Si-RNA transfection (sc-35969, Santa Cruz). Overexpression of MSH2 was produced by transfecting the vector pCMV6-AC (Origene), which contains the human MSH2 cDNA sequence. Overexpression of mutant MRE11 was achieved by transfection of pIRES-MRE115Δ7 (a kind gift from Mark Meuth,

University of Sheffield, UK) Transfections were performed using Nucleofection (Lonza, Switzerland) according to the manufacturer's instructions. Transient knockdown of CtIP expression in leukemia cells was achieved by Si-RNA transfection (L-011376-00-0005), ON-TARGET plus SMART pool (Dharmacon, Lafayette, CO, USA) and sc-37765, (Santa Cruz). Stable overexpression of CtIP was prepared through transfection of pZGFP-C1-CtIP containing wild-type CtIP cDNA (a kind gift from Penny Jeggo, University of Sussex, UK). Cell lines stably transfected with pGFP-V-RS were continually selected in 1  $\mu$ g/mL puromycin. Cell lines stably transfected with pCMV-AC were continually selected in 500  $\mu$ g/mL G418. Transient knockdown of BRCA2 expression in leukemia cells was achieved by Si-RNA transfection (sc-35969, Santa Cruz) and ON-TARGET plus SMART pool - Human BRCA2 (L003462-00-0005, Dharmacon) and sc-29825, Santa Cruz).

### Statistical analyses

Two-tailed Student's t-tests were conducted to compare viability analysis and Rad51/phospho-H2AX foci in MSI positive and

**Table 1.** Correlation of MSI and HR competency in MDS/AML cell lines and AML patients.

| MDS/AML patients and cell Lines | MSI Panel |      |      |       |       |        | DNA repair genes |     |       |           |           |     |      |      |          |       |      |       |      |       | HR |         |   |
|---------------------------------|-----------|------|------|-------|-------|--------|------------------|-----|-------|-----------|-----------|-----|------|------|----------|-------|------|-------|------|-------|----|---------|---|
|                                 | NR21      | NR22 | NR24 | BAT25 | BAT26 | MONO27 | ATM              | ATR | BRCA1 | BRCA2 (9) | BRCA2(22) | BLM | CHK1 | CtIP | DNA-PKcs | MRE11 | PTEN | PARP1 | TNK1 | RAD50 |    | TGF-βII |   |
| KG-1                            | ◦         | ◦    | •    | ◦     | ◦     | ◦      | ◦                | •   | •     | •         | •         | •   | •    | ◦    | •        | ◦     | •    | •     | •    | •     | •  | X       | • |
| Molm-13                         | ◦         | ◦    | •    | ◦     | ◦     | ◦      | ◦                | •   | •     | •         | •         | •   | ◦    | ◦    | •        | ◦     | •    | •     | •    | •     | •  | X       | • |
| NB4                             | ◦         | ◦    | •    | ◦     | ◦     | ◦      | ◦                | •   | •     | •         | •         | •   | ◦    | ◦    | •        | ◦     | •    | •     | •    | •     | •  | X       | • |
| OCI-AML2                        | •         | •    | •    | •     | •     | •      | •                | •   | •     | •         | •         | •   | •    | •    | •        | •     | •    | •     | •    | •     | •  | •       | • |
| OCI-AML3                        | •         | •    | •    | •     | •     | •      | •                | •   | •     | •         | •         | •   | •    | •    | •        | •     | •    | •     | •    | •     | •  | •       | • |
| P39                             | ◦         | ◦    | •    | ◦     | ◦     | ◦      | ◦                | •   | •     | •         | •         | •   | •    | ◦    | •        | ◦     | •    | •     | •    | •     | •  | •       | • |
| AML 1                           | •         | •    | •    | •     | •     | •      | •                | •   | •     | •         | •         | •   | •    | •    | •        | •     | •    | •     | •    | •     | •  | X       | • |
| AML 2*                          | ◦         | •    | ◦    | •     | ◦     | ◦      | •                | •   | •     | •         | •         | •   | •    | •    | •        | ◦     | •    | •     | •    | •     | •  | X       | • |
| AML 3                           | •         | •    | •    | •     | •     | •      | •                | •   | •     | •         | •         | •   | •    | •    | •        | •     | •    | •     | •    | •     | •  | X       | • |
| AML 4                           | •         | •    | •    | •     | •     | •      | •                | •   | •     | •         | •         | •   | •    | •    | •        | •     | •    | •     | •    | •     | •  | X       | • |
| AML 5                           | ◦         | •    | •    | •     | •     | ◦      | •                | •   | •     | •         | •         | •   | •    | ◦    | •        | •     | •    | •     | •    | •     | •  | X       | • |
| AML 6                           | •         | •    | •    | •     | •     | •      | •                | •   | •     | •         | •         | •   | •    | •    | •        | •     | •    | •     | •    | •     | •  | •       | • |

Microsatellite loci were analyzed by fluorescent fragment PCR. MSI panel PCR products with  $\geq 3$ bp are considered MSI positive. Bi-allelic MSI panel deletions ( $\geq 3$ bp) are indicated as open circles (◦). Closed circles (•) indicate no MSI (MSI panel PCR products  $< 3$ bp) or no deletions in DNA repair gene microsatellites. ◦ indicate the presence of mono-allelic MSI panel PCR products or mono-allelic DNA repair gene microsatellite deletions. For HR competency, HR dysfunction is indicated as crosses. Therapy-related AML (t-AML) patients are indicated by an asterisk (\*).

negative MDS/AML. Fisher's exact tests were used to compare MSI positivity and chromosomal instability. Analyses were calculated using Graphpad™. A one-way ANOVA was performed for gene expression studies and *P* value cut offs were determined by Bonferroni's multiple test correction with the threshold set at 0.05.

Further details of Design and Methods are available in the *Online Supplementary Appendix*.

## Results

### MSI mutates DNA repair genes in MDS/AML

To correlate MSI with the abrogation of double strand DNA repair we analyzed the lengths of 6 mononucleotide repeat markers using fluorescent fragment PCR in 12 MDS/AML cell lines. This panel of microsatellite markers has been shown to accurately evaluate MSI status without the need to match germ-line DNA.<sup>15</sup> In contrast, dinucleotide microsatellites have been documented to show instability in 60-80% of MSI-High cancers whilst there is evidence for mis-classification when using such repeats.<sup>16,17</sup> Four of 12 (33%) MDS/AML cell lines including the myelomonocytic/myelodysplastic cell line, P39, AML cell lines, Molm-13 and KG-1 and the acute promyelocytic leukemic cell line, NB4 also exhibited high-grade MSI ( $\geq 2$  shortened loci with  $\geq 3$  nucleotide errors) (Table 1, *Online Supplementary Table S2*, *Online Supplementary Figure S2A and B*). Furthermore, 2 of 18 (11%) primary AML samples (t-AML Patient 2 and de novo AML Patient 5) were MSI-High (Table 1, Figure 1A and B, *Online Supplementary Tables S2-3*).

We then sequenced the coding region mononucleotide repeats within the DNA repair genes *BLM*, *ATR*, *DNA-PK*, *ATM*, *MRE11*, *CtIP*, *RAD50*, *CHK1*, *BRCA1*, *BRCA2*, *PARP1*, *TNK1* and *PTEN* and in the gene, *TGF-βII* in primary AML cells and MDS/AML cell lines. No coding

region microsatellite mutations were observed in *RAD50*, *CHK1*, *BRCA2*, *BLM*, *ATR*, *DNA-PK*, *RAD50*, *BRCA1*, *PARP1*, *TNK-1*, *PTEN* and *TGF-βII* genes in either MSI positive or negative MDS/AML cell lines or primary AML (Table 1, *Online Supplementary Tables S2-S3*). However, AML Patient 2 exhibited a 1 bp mono-allelic mutation of the poly (T)11 microsatellite in the intronic region between exon 4 and 5 of *MRE11* (Figure 1C). AML Patient 5 exhibited a mono-allelic 1bp mutation of the poly (T)9 nucleotide repeat in exon 11 of *CtIP* (Figure 1D). Moreover, 1-2 bp coding region microsatellite mutations in *MRE11*, *CtIP* and *ATM* were seen in the MSI positive cell lines, P39, Molm-13, KG-1 and NB4 cells (*Online Supplementary Table S2*, *Online Supplementary Figure S2A-D*). No mutations in *MRE11*, *CtIP* and *ATM* were observed in MSI negative MDS/AML cell lines, primary AML cells, or normal peripheral blood lymphocytes (PBL) (*Online Supplementary Tables S2-S3*, *Online Supplementary Figure S2A-D*). Mononucleotide repeat mutations generated splicing variants in DNA repair genes. Intronic deletions between exons 4 and 5 in *MRE11* results in 88bp deletion removing exons 5-7, whilst intronic deletions in *ATM* between exons 7 and 8 results in a 22bp deletion removing exon 8. PCR amplification of the cDNA containing exon 5 of *MRE11* revealed that MSI positive primary AML Patient 2 exhibited aberrant splicing products compared to AML Patient 5 (MSI positive) and MSI negative patients (ratio of intensity (RI), mean 0.4 vs. 0.175, two-tailed Student's *t*-test, *P*>0.05) (Figure 1E). MSI positive cell lines P39, Molm-13, KG-1 and NB4 also exhibited aberrant splicing products for exon 5 of *MRE11* and exon 8 of *ATM* (*Online Supplementary Figure S3A and B*).

FLAG-tagged *MRE115A7* was transfected into MSI negative cell line, U937. The faster migrating form of mutant *MRE11* was confirmed to be *MRE115A7* through detection by anti-FLAG (*Online Supplementary Figure S4*).

**Table 2. Correlation of MSI positivity and chromosomal instability in MDS patients.**

| MD  | MSI Panel |      |      |       |       |        | DNA repair genes |     |       |           |            |     |      |      |          |       |      | Chromosomal instability |      |       |         |            |                                   |             |
|-----|-----------|------|------|-------|-------|--------|------------------|-----|-------|-----------|------------|-----|------|------|----------|-------|------|-------------------------|------|-------|---------|------------|-----------------------------------|-------------|
|     | NR21      | NR22 | NR24 | BAT25 | BAT26 | MONO27 | ATM              | ATR | BRCA1 | BRCA2 (9) | BRCA2 (22) | BLM | CHK1 | CtIP | DNA-PKcs | MRE11 | PTEN | PARP1                   | TNK1 | RAD50 | TGF-βII | CNC (Chr.) | CN-LOH/UPD (Chr.)                 |             |
| 1   | °/●       | ●    | ●    | ●     | ●     | ●      | ●                | ●   | ●     | ●         | ●          | ●   | ●    | ●    | ●        | ●     | ●    | ●                       | ●    | ●     | ●       | ●          | ND                                | 11          |
| 2   | ●         | °/●  | °/●  | ●     | ●     | ●      | ●                | ●   | ●     | ●         | ●          | ●   | ●    | °/●  | ●        | ●     | ●    | ●                       | ●    | ●     | ●       | ●          | 5,7                               | 2           |
| 3   | ●         | ●    | ●    | ●     | ●     | /●     | ●                | ●   | ●     | ●         | ●          | ●   | ●    | ●    | ●        | ●     | ●    | ●                       | ●    | ●     | ●       | ●          | ND                                | 11          |
| 4   | °/●       | ●    | ●    | ●     | ●     | ●      | ●                | ●   | ●     | ●         | ●          | ●   | ●    | ●    | ●        | ●     | ●    | ●                       | ●    | ●     | ●       | ●          | 7                                 | ND          |
| 5   | °/●       | ●    | ●    | ●     | °/●   | ●      | ●                | ●   | ●     | ●         | ●          | ●   | ●    | °/●  | ●        | ●     | ●    | ●                       | ●    | ●     | ●       | ●          | ND                                | 2,4,9<br>19 |
| 6   | ●         | ●    | °/●  | ●     | ●     | ●      | ●                | ●   | ●     | ●         | ●          | ●   | ●    | ●    | ●        | ●     | ●    | ●                       | ●    | ●     | ●       | ●          | 7,9,18<br>20,21                   | ND          |
| 7   | ●         | ●    | °/●  | °/●   | ●     | ●      | ●                | ●   | ●     | ●         | ●          | ●   | ●    | °/●  | ●        | ●     | ●    | ●                       | ●    | ●     | ●       | ●          | 1,6,7,9                           | 9           |
| 8   | °/●       | ●    | ●    | ●     | ●     | ●      | ●                | ●   | ●     | ●         | ●          | ●   | ●    | ●    | ●        | ●     | ●    | ●                       | ●    | ●     | ●       | ●          | 21                                | 20          |
| 9   | ●         | ●    | °/●  | ●     | ●     | ●      | ●                | ●   | ●     | ●         | ●          | ●   | ●    | ●    | ●        | ●     | ●    | ●                       | ●    | ●     | ●       | ●          | 7,9                               | 6           |
| 10  | °/●       | ●    | ●    | ●     | ●     | ●      | ●                | ●   | ●     | ●         | ●          | ●   | ●    | ●    | ●        | ●     | ●    | ●                       | ●    | ●     | ●       | ●          | 3,7,18                            | 21          |
| 11  | °/●       | ●    | ●    | ●     | °/●   | ●      | ●                | ●   | ●     | ●         | ●          | ●   | ●    | °/●  | ●        | ●     | ●    | ●                       | ●    | ●     | ●       | ●          | 1,4,5,<br>7,12,<br>16,17<br>20,21 | ND          |
| 12* | ●         | ●    | ●    | ●     | °/●   | ●      | ●                | ●   | ●     | ●         | ●          | ●   | ●    | ●    | ●        | ●     | ●    | ●                       | ●    | ●     | ●       | ●          | 7                                 | 13          |
| 13* | ●         | ●    | ●    | ●     | ●     | ●      | ●                | ●   | ●     | ●         | ●          | ●   | ●    | ●    | ●        | ●     | ●    | ●                       | ●    | ●     | ●       | ●          | 5,6,7,<br>18,21                   | 1           |

Microsatellite loci were analyzed by fluorescent fragment PCR. MSI panel PCR products with  $\geq 3bp$  are considered MSI positive. Bi-allelic MSI panel deletions ( $\geq 3bp$ ) are indicated as open circles (°). Closed circles (●) indicate no MSI (MSI panel PCR products  $< 3bp$ ) or no deletions in DNA repair gene microsatellites. °/● indicate the presence of mono-allelic MSI panel PCR products or mono-allelic DNA repair gene microsatellite deletions. For HR competency, HR dysfunction is indicated as crosses. Therapy related AML (t-AML) patients are indicated by an asterisk. For chromosomal instability, chromosomal location is given for copy number changes (CNC) (losses and gains) and acquired copy neutral LOH/UPD were determined by SNP analysis. ND- not detected. Therapy-related MDS (t-MDS) patients are indicated by an asterisk (\*).

Western blotting with anti-MRE11 also identified a faster migrating form of MRE11 appearing at a similar molecular weight (70kDa) in MSI positive primary AML 2 cells and in MDS/AML cell lines (Figure 1F). A 1 bp deletion within the coding exon of CtIP produces a frame-shift mutation that creates a severely truncated protein that removes amino acids 328-897. Western blotting using an antibody recognizing the C-terminal of CtIP confirmed a 2-fold reduction in CtIP expression, using quantitative measurement of band intensity (Figure 1F and G), in AML Patient 5 and the MDS/AML cell lines KG-1, Molm-13, P39 and NB-4. However, due to the absence of an effective N-terminal CtIP antibody, we could not entirely rule out the presence of an N-terminal 1-327 amino acid truncated CtIP protein.

Lack of a functional mismatch repair (MMR) pathway has been shown to be instrumental in inducing MSI.<sup>3</sup> Primary AML cells, MDS/AML cell lines and the MSI positive colon cancer cell line, LoVo were probed for expression of PMS2, MLH1, MSH-2, MLH3 and MSH6 by Western blotting (Figure 1H and I). MSI positive AML Patient 2 and Patient 5 showed a 2-3 fold reduction in expression of MSH2 and MLH1, respectively. MSI negative AML patients did not demonstrate loss of MMR protein expression. MSI positive MDS/AML cell lines, KG-1 and Molm-13 and P39 demonstrated a 2-3 fold reduction

in MSH2 and MLH6 expression whilst NB4 showed a loss of MLH1. MSI negative cell lines did not exhibit any changes in the expression of MMR proteins.

### MSI positivity inhibits HR and confers PARP inhibitor sensitivity in MDS/AML

Poly ADP-ribose polymerase inhibitors (PARPi) specifically target cells with DSB DNA repair defects. We determined that the 2 MSI positive primary AML cell samples, as well as the MDS/AML cell lines, P39, AML cell lines, Molm-13 and KG-1 and the acute promyelocytic leukemic cell line, NB4 demonstrated aberrant cell cycle profiles, decreased viability and increased apoptosis following culture in the presence of the PARPi, BMN 673 (Online Supplementary Figures S5 A,C and S6). BMN 673 exerted the greatest PARP inhibitory activity in comparison to other PARPi and exerted extreme cytotoxicity to BRCA2 silenced K562 cells (Online Supplementary Figure S7), and was the PARPi of choice in subsequent studies. Three other AML patient samples that were MSI negative were also HR defective and sensitive to BMN673; however, HR competent/PARPi insensitive primary AML and MDS/AML cell lines did not demonstrate MSI (Online Supplementary Tables S2-S3). Cells from the 2 MSI positive AML patients and the MSI positive P39, KG-1, Molm-13 and NB4, also showed increased phospho-γH2AX foci by

immunofluorescence studies and a marked reduction in rad51 foci formation in response to PARPi indicating defective homologous recombination (HR) mediated DNA repair. (Online Supplementary Figures S5 D,E and S8, two-tailed Student's t-test,  $P < 0.05$ ,  $n = 3$ ). However, the low level rad51 foci formed in mutant MRE11 and CtIP cells co-localizes with cyclin A positive cells and thus predominates in the S/G2 fraction of the cell cycle akin to the unmutated MRE11 and CtIP in Patient 6 (Online Supplementary Figure S9). PARPi cytotoxicity in MDS/AML cells was dependent on HR competence and not on the levels of intrinsic PARP activity between samples, in accordance with our previous study of primary AML9 (Online Supplementary Figure S10). PARP activity was determined by measuring endogenous poly ADP-ribose (PAR) formation with and without stimulation by DNA strand breaks and we show that PARPi sensitive and insensitive MDS/AML cell lines had similar PARP activities (1.2-1.7 and 39-85 nmol/10<sup>6</sup> cells) (Online Supplementary Table S4). BMN 673 inhibited PARP activity with an IC<sub>50</sub> of less than 5 nM in all MDS/AML cell lines tested.

### Association of MSI with chromosomal instability in high risk MDS

We have previously identified defects in the DNA DSB repair pathway in hematologic disorders that have the potential to drive chromosomal instability.<sup>7</sup> Hence, we looked for an association between MSI and chromosomal instability. MDS is not only associated with gross chromosomal instability, but also displays acquired uniparental disomy (UPD). Thirteen of 63 (21%) MDS patients exhibited MSI (9 MSI-Low and 4 MSI-High) (Figure 2A, Online Supplementary Tables S5 and S6). Five of 63 patients were therapy-related MDS (t-MDS) and 2 of these 5 were MSI positive indicating that 11 of 13 (4 MSI-High, 7 MSI-Low) were *de novo* MDS patients. Repetitive analysis for each patient excluded PCR artifacts as a source of instability at individual loci. Moreover, germ-line constitutional DNA from these 63 patients did not exhibit MSI (*data not shown*) suggesting that the MSI-Low group constitutes a genuine MSI phenotype. Of the 13 MSI positive patients, 8 of 13 (4 MSI-High, 4 MSI-Low) had monosomy 7 and other complex chromosomal abnormalities (62%), 2 of 13 (MSI-Low) patients had isolated monosomy 7 (15%) whilst 3 of 13 patients (MSI-Low) had normal metaphase cytogenetics (MC) (23%). TP53 sequencing revealed that 15 of 63 (24%) possessed TP53 mutations (Online Supplementary Table S6). However, from 24 MDS patients who had complex cytogenetics, 15 of 24 (62%) had mutated TP53. In contrast, MSI is found in 7 of 24 patients with complex cytogenetics (29%). Moreover, 3 of 4 MSI-High MDS patients had wild-type TP53. Of the 63 MDS patients, only 3 MDS patients possessed acquired UPD as their sole chromosomal abnormality and these 3 patients demonstrated MSI (Online Supplementary Tables S5 and S6). Of note, in 17 (27%) patients with normal metaphase cytogenetics and a normal SNP-A karyotyping profile, MSI was not demonstrated (Fisher's exact test, two-tailed  $P = 0.02$ ). Moreover, from the MSI positive cohort, 9 of 13 (69%) have LOH/UPD chromosomal changes in contrast to MSI negative patients (6 of 50, 12%). Four patients with *de novo* high-grade MSI demonstrated the presence of a mono-allelic 1 bp deletion in the CtIP exon coding microsatellite (Figure 2B). None of the MSI positive and MSI negative MDS patients showed coding region mononucleotide

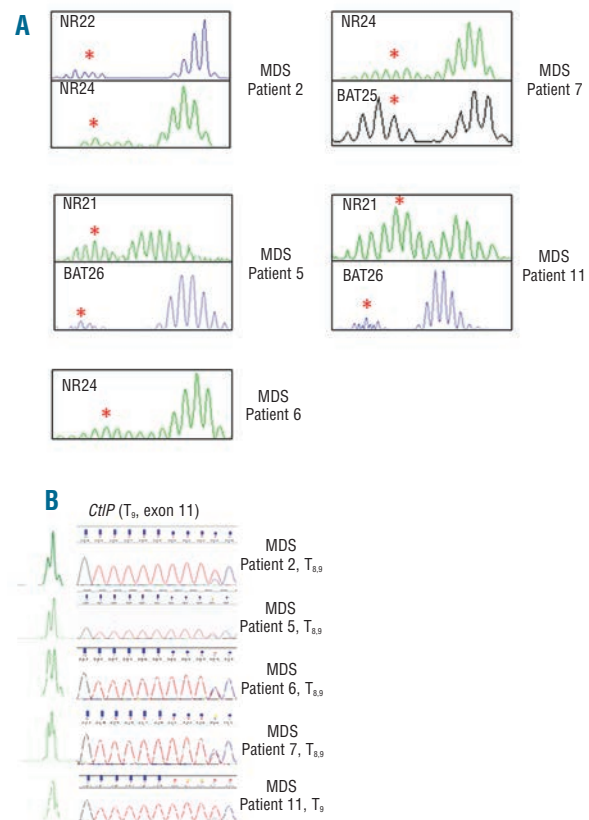


**Figure 2.** Identification of MSI positivity in patients with high risk MDS. (A). MSI loci profiles using fluorescent fragment PCR for NR24, (upper panel) NR21 (middle panel) and BAT26 (lower panel) microsatellites showing heterozygous deletions in DNA from MDS patient 2 and patient 5. Asterisks indicate presence of significantly shortened microsatellite species. (B). Fluorescent fragment PCR and Sanger sequencing of the DNA repair gene CtIP exon 11 microsatellite. DNA from primary MDS was used in PCR reactions for CtIP reactions, (9 thymine microsatellite T9, exon 11). Fluorescent fragment profile is shown in left panel, Sanger sequence is shown in right panel.

microsatellite mutations in *MRE11*, *ATM*, *BLM*, *ATR*, *RAD50*, *CHK1*, *BRCA2*, *BRCA1*, *PTEN*, *TNK1*, *DNA-PKcs*, *PARP1* and *TGF-βII* (Online Supplementary Tables S5 and S6). No significant correlation between MSI and the blast percentage in the marrow could be made. Additionally, no significant correlations could be made between MSI and cytopenia or IPSS risk categories of MDS (*data not shown*).

### Disruption of MMR function alone does not disrupt HR responses

To determine whether sensitivity to PARPi is attributable to MSI-induced DNA repair gene mutations, rather than solely to a defect in MMR, we used short hairpin (SH-RNA) and Si-RNA to silence the expression of MSH2 in the MMR competent (MSI negative) cell line U937 (Figure 3A-B,G, Online Supplementary Figure S11A-E). Reduced expression of MSH2 exhibited a negligible effect on HR activity in response to PARP inhibition. MSI analysis revealed no microsatellite mutations in the MSI and DNA repair gene panels in MSH2 silenced U937 (Online Supplementary Table S2). Moreover, transfection of an MSH2 over-expressing vector into P39 cells did not affect HR responses (Figure 3G, Online Supplementary Figure S11F-H). In addition, reduced expression or overexpres-

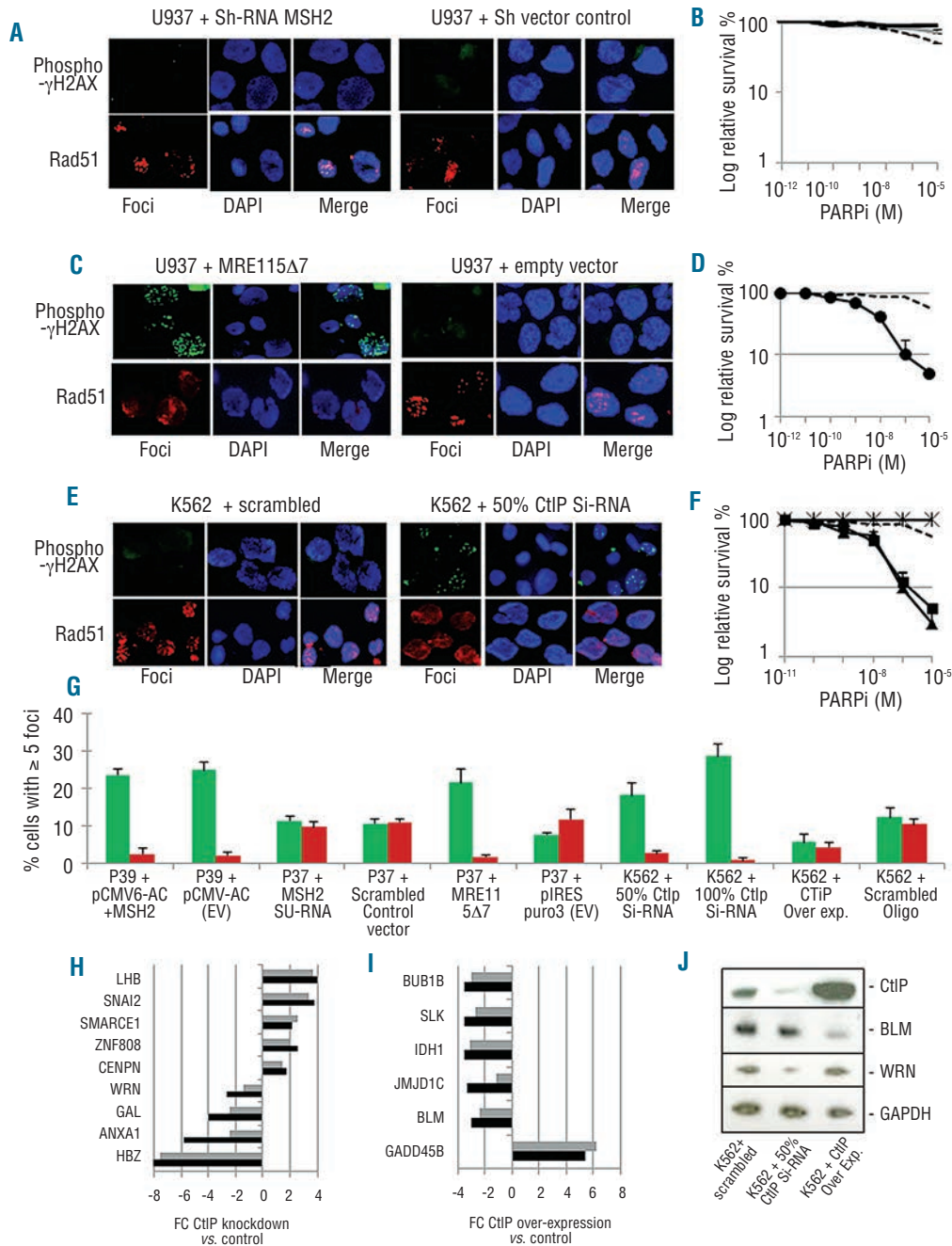


**Figure 3.** HR responses after modulation of the MMR pathway, MRE11 mutation and CtIP expression. (A-B) Modulation of HR by PARPi after MSH2 reduction. **A.** Representative rad51 and phospho-H2AX foci in U937 + pooled Sh-RNA MSH2 (left panel) and U937 + scrambled control vector (right panel) after treatment with 100nM PARPi for 24h, **B.** U937 + pooled MSH2 Sh-RNA (solid line), U937 + Si-RNA (gray line), U937 + scrambled control vector (dashed line). PARPi was incubated for 120 h before plating on soft agar for 14 days. (C-D). Mutant MRE11 confers dysfunctional HR. U937 was transfected with mutant MRE115 $\Delta$ 7. **C.** Representative rad51 and phospho- $\gamma$ H2AX foci after treatment with PARPi for 24 h in U937 + MRE115 $\Delta$ 7 (left panel) and U937 + empty vector (right panel). **D.** U937 was transfected with mutant MRE11 5 $\square$ 7 treated with PARPi (MRE115 $\Delta$ 7, solid line, circles) or empty vector + PARPi (dashed line) for 120 h before plating on soft agar for 14 days. (E and F). Differential expression of CtIP modulates HR and PARPi sensitivity. Representative rad51 and phospho- $\gamma$ H2AX foci after treatment with 100 nM PARPi for 24 h in K562 + scrambled oligo (left panel) and K562 + 50% (16nM) CtIP Si-RNA (Dharmacon, right panel). **F.** PARPi was added 24 h after Si-RNA transfection and incubated for a further 120 h before plating on soft agar for 14 days. 50% (17nM) CtIP Si-RNA silencing (Dharmacon, diamonds) or 50% (19nM) CtIP RNA silencing, (Santa Cruz, squares) CtIP Si-RNA, over-expression vector, pZGFP-C1-CtIP (crosses) or with scrambled control (dashed line). **G.** Frequency of phospho- $\gamma$ H2AX foci positive cells (%) (green bars) and rad51 foci positive cells (%) (red bars) following 24 h PARPi addition. Error bars represent the means  $\pm$  S.E.M. of three separate experiments. (H-I). Gene expression profiling after differential expression of CtIP. Expression profiles of CtIP silenced K562 treated with 100 nM PARPi for 24 h vs. K562 transfected with scrambled control treated with 100 nM PARPi for 24 h (H) and K562 + CtIP over-expressed treated with 100 nM PARPi for 24 h vs. K562 transfected with scrambled control treated with 100 nM PARPi for 24 h (I). Differentially expressed DNA damage signaling/mitosis/chromatin remodeling genes are indicated. FC, Fold change. Q-PCR (gray bars), Affymetrix (black bars), FC gene expression. (J). Expression of CtIP, WRN and BLM in K562 + 50% (17nM) CtIP Si-RNA (Dharmacon), K562 + CtIP over-expressed and K562 + scrambled control. GAPDH acted as an immunoblot loading control. The immunoblots shown are representative of 3 independent experiments.

sion of MSH2 exhibited a negligible effect on PARPi cytotoxicity (Figure 3B, *Online Supplementary Figure S11 I*).

### **Mutant MRE11 lacking exon 5-7 and the silencing of CtIP expression confer HR inhibition**

*MRE11*, with deletion of exons 5-7 has previously been shown to act in a dominant negative manner inducing sensitivity to camptothecin.<sup>18</sup> Transfection of mutant *MRE11Δ7* into U937 induced a negative impact on HR repair demonstrated by increased phospho- $\gamma$ H2AX foci and decreased rad51 foci compared to U937 + empty vector after PARPi addition and a significant increase in PARPi cytotoxicity (Figure 3C-D,G, two-tailed Student's t-test,  $P < 0.05$ ,  $n=3$ ). Similarly, 50% reduction of CtIP expression in the MSI negative CML cell line, K562 to equivalent levels observed in AML Patient 5 and in cell lines KG-1, NB4 and molm-13 inhibited HR responses and conferred PARPi cytotoxicity. (Figure 1G, Figure 3E-G, *Online Supplementary Figure S12A-D,F*). However, 100% CtIP knockdown resulted in complete abrogation of HR competence, and had a detrimental effect on cell viability without drug, and so PARPi sensitivity could not be analyzed in such cells. Conversely, overexpression of CtIP caused reduced DSB DNA damage in response to PARPi (Figure 3G, *Online Supplementary Figure S12E*, two-tailed Student's t-test,  $P < 0.05$ ,  $n=3$ ). Moreover, overexpression of CtIP significantly reduces sensitivity to PARPi (Figure 3F).

### **Delineation of CtIP mutant 'signature'**

Lastly, as CtIP was mutated in a number of MDS/AML patients with chromosomal instability, we attempted to identify the *CtIP* gene expression 'signature' comparing expression profiles of Si-RNA silenced *versus* over-expressed CtIP. K562 cells were transfected with either Si-RNA to CtIP, CtIP over-expressing plasmid, pZGFP-C1-CtIP or scrambled oligonucleotide control, and incubated for 24 h with PARPi. We found 217 genes that were differentially expressed in the CtIP Si-RNA silenced *versus* scrambled oligonucleotide profile and 177 genes differentially expressed in the CtIP over-expressed *versus* scrambled oligonucleotide profile. Figure 3H-I shows the DNA repair, cell cycle and chromatin regulating genes from each profile. These genes were found in the top 60 differentially expressed genes with the greatest fold change. RNA silencing of CtIP in the presence of PARPi dramatically reduces the expression of the RecQ helicase, WRN (fold change (FC) -2.7, unadjusted  $P < 0.03$ ). Moreover, the over-expression of CtIP in the presence of PARPi significantly reduces the expression of another RecQ helicase, BLM (FC -3.3, adjusted  $P < 0.0001$ ). Quantitative PCR (Q-PCR) (Figure 3H and I) and Western blotting (Figure 3J) confirmed the modulation in expression of WRN and BLM.

## **Discussion**

In this report, we show that defects in the MMR pathway cause MSI in the myeloid cancers, such as MDS and AML. In turn, MSI-dependent mutations in the DNA repair genes, MRE11 and CtIP, perturb DSB DNA repair pathways. The phenomenon of MSI is found in 10-15% of colorectal cancers and is believed to be a key event in colorectal tumor genesis.<sup>3</sup> MSI is divided into two distinct types: MSI-High tumors have a definitive clinical phenotype and are associated with an MMR defect. In contrast, the phenotype, biological basis and validity of MSI-Low

tumors remain uncertain.<sup>19</sup> Several reports, however, have established the existence of MSI-Low in a number of different cancers in addition to colon tumors arguing that MSI-Low represents an intermediate between MSI-High and microsatellite stable (MSS) tumors.<sup>20,21</sup> MSI (High and Low) have been previously documented to be a rare occurrence in *de novo* hematologic malignancies and reports on MSI positive MDS/AML are confined to cases secondary to alkylating agent therapy.<sup>22,23</sup> However, the use of systematic and stringent sequencing measures to identify low clone MSI species determined 20% MSI positive *de novo* MDS suggesting that the importance of MSI in leukemic progression requires re-evaluation. Consistent with the 'mutator phenotype' theory proposed by Loeb,<sup>2</sup> the acquisition of MSI/MMR deficiency induces a high mutation rate providing the mutations required for adaptation, evolution of the tumor cells and disease progression. All 13 MDS patients with MSI in our study exhibited chromosomal instability, whilst a further 15 MDS patients without MSI exhibited no chromosomal abnormality, suggesting that MSI/loss of MMR confers an increased propensity to develop the chromosomal instability phenotype. Indeed, a significant correlation was made between the MSI-Low phenotype and LOH in early colorectal cancers.<sup>24</sup> Chromosomal instability such as acquired UPD, in turn conveys further genomic changes conducive to leukemic progression.

Although we make the significant correlation between MSI and chromosomal instability, a sizeable majority of samples that had chromosomal changes were MSI negative, suggesting there are other mechanisms that contribute to the chromosomal instability in MDS/AML. Similarly, other mechanisms confer PARPi sensitivity in our AML cohort. The acquisition of TP53 mutations is mainly observed in high-risk and therapy-related MDS associated with complex karyotypes.<sup>25</sup> Complex chromosomal instability in the MDS cohort was correlated with TP53 mutations and not MSI. Conversely, the MSI positive cohort was greatly correlated with LOH/UPD chromosomal changes, suggesting that MSI may predispose for the LOH/UPD phenotype rather than the complex cytogenetic phenotype associated with TP53. Moreover, TP53 mutations may also co-operate with the MSI-Low phenotype to exacerbate the complex karyotype. Indeed, 3 of the 4 MSI-High MDS patients had wild-type TP53, suggesting that the more aggressive MSI-High phenotype alone can confer the complex karyotype. MSI may also turn out to be tissue specific. In colon cancer, microsatellite mutations in the gene for type II TGF- $\beta$  receptor is the most common consequence and a direct cause of the malignant phenotype.<sup>1</sup> In contrast, we failed to observe TGF- $\beta$ II microsatellite mutations in MDS/AML. Therefore, it is likely that each cancer cell type uses a distinct developmental pathway in its disease progression.

MMR deficiency has also been shown to modulate drug sensitivity.<sup>13,14</sup> Base analogs such as cytarabine (Ara-C) and fludarabine are thought to generate DNA lesions that stall replication forks.<sup>26</sup> These lesions are recognized and removed by the MMR apparatus, therefore defective MMR synergizes with these anti-leukemia agents. Our data suggest that, whilst cytotoxicity due to PARPi is dependent on the failure to restart stalled replication forks, the MMR pathway is not activated by PARPi challenge. Therefore, a loss of MMR activity is not sufficient to provide PARPi sensitivity, without the preceding mutations in

the DNA repair genes caused by the MMR/MSI defect. Conversely, the base analog thiopurine and methylating agents such as N-methyl-N-nitrosourea (MNU) generate DNA lesions that are recognized and directed to cell death by the MMR apparatus.<sup>27,28</sup> In this case, MMR deficiency confers resistance to thiopurine and MNU. Conceivably then, in our leukemic model, acquisition of MSI/MMR deficiency confers a phenotype conducive to leukemic expansion, but also acts to protect the leukemic stem cell clone from the effects of some of the chemotherapeutic agents. However, paradoxically the very same mechanism that confers resistance to mutagenic insults inadvertently 'opens the door' for alternative therapies. The intronic splice acceptor mutation between intron 4/exon 5 in MRE11 and intron 7/exon 8 in ATM have been previously shown in colon tumors.<sup>29,30</sup> However, we are the first to report novel frame-shift mono-allelic microsatellite mutation in MRE11, ATM and CtIP in primary MDS/AML and cell lines. MRE11 possesses both exonuclease and endonuclease activities and functions in the recognition and resection of DNA DSB, the cell cycle checkpoint and replication re-start after fork collapse.<sup>31,32</sup> Mutant MRE11 (deleted exons 5-7, MRE11 5Δ7) codes for a protein that retains DNA binding activity but that has lost its exonuclease activity and which competes with wild-type MRE11 for DNA binding.<sup>18</sup> Similarly, CtIP is also involved in DNA DSB end resection thus regulating repair by HR.<sup>31</sup> CtIP is also a target for BRCA1 dependent phosphorylation by ATM after DNA DSB damage whilst haploinsufficiency of CtIP results in tumorigenesis.<sup>33-35</sup> We show that both dominant negative MRE115Δ7 and reduced CtIP expression compromise HR DNA repair and render the cells sensitive to PARPi. Other DNA DSB repair genes, such as Rad50 and ATR, were not mutated in our study. This suggests that reduced expression of ATM, MRE11 or CtIP generates chromosomal instability, but also allows leukemic cell survival and growth, unlike mutations in Rad50 and ATR. In this respect, it is worth noting that complete RNA-silencing of CtIP was not conducive to prolonged viability. In addition to its role in DNA DSB repair, we note that CtIP associates with RB1 and is thus required for the G<sub>1</sub>/S phase transition. Evidently, at least some CtIP expression is required to allow cells to enter the S-phase.<sup>36</sup> Heterozygous expression of CtIP in the PARPi sensitive AML patient was conducive to normal cell cycle kinetics, as shown by the similar distribution of cyclin A compared to the unmutated CtIP patients. This suggests that PARPi sensitivity as a result of a CtIP mutation is due to a DNA

repair anomaly rather than cell cycle abnormalities. Interestingly, the overexpression of CtIP increased the resistance to PARPi. Increased diversion of DNA DSB repair from the error-prone Non Homologous End-Joining (NHEJ) pathway to error-free HR repair should, in theory, reduce PARPi-induced chromosomal instability and hence promote viability. Moreover, as CtIP over- and under expression directly correlates with HR processing activity, this suggests that CtIP expression is rate limiting for HR. We further implicate CtIP as a mediator of genomic stability through its modulation of RecQ helicases, BLM and WRN. These helicases act to dissolve illegitimate HR intermediates and abrogation of their activity results in increased and inappropriate HR events.<sup>37</sup> Acquired UPD has been proposed to be caused by de-regulated mitotic recombination, associated with defects in several components of DNA HR repair. Therefore, we suggest that mutations in genes, such as CtIP, could play a key role in generation of acquired UPD. Indeed, in our cohort of MDS patients, in whom acquired UPD was the sole chromosomal abnormality, we have observed that these patients demonstrated MSI and one patient exhibited a CtIP microsatellite mutation.

In conclusion, the MSI phenotype confers hypersensitivity to PARPi through perturbation of DSB repair pathways in cancer. During the last few years the clinical efficacy of using PARPi has focused on exploiting mutant BRCA alleles in breast and ovarian cancers. This represents a minority of cancers. The challenge now is to broaden the applicability of PARPi, in the knowledge that genomic instability is far more prevalent in cancer than the presence of BRCA mutations. With the inaugural phase I clinical trial for the treatment of MDS/AML at King's College, London, UK, actively recruiting patients (*ClinicalTrials.gov Identifier: NCT01399840*), the identification of MRE11 and CtIP mutations, confirms that PARPi can be synthetically lethal in MDS/AML patients who bear these particular mutations, signifying a major development in identifying candidates for PARPi therapy.

#### Funding

This work was funded by King's College Hospital, London, UK.

#### Authorship and Disclosures

Information on authorship, contributions, and financial & other disclosures was provided by the authors and is available with the online version of this article at [www.haematologica.org](http://www.haematologica.org).

## References

- Kolodner RD. Mismatch repair: mechanisms and relationship to cancer susceptibility. *Trends Biochem Sci.* 1995;20:397-401.
- Loeb LA, Springgate CF, Battula N. Errors in DNA replication as a basis of malignant changes. *Cancer Res.* 1974; 34: 2311-21.
- Hampel H, Frankel WL, Martin E, Arnold M, Khanduja K, Kuebler P, et al. Screening for the Lynch syndrome (hereditary nonpolyposis colorectal cancer). *N Engl J Med.* 2005;352:1851-60.
- Morgan MA, Reuter CW. Molecularly targeted therapies in myelodysplastic syndromes and acute myeloid leukemias. *Ann Hematol.* 2006;85(3):139-63.
- Hirst WJ, Czepulkowski B, Mufti GJ. Consistent interstitial chromosomal deletions in myeloid malignancies and their correlation with fragile sites. *Cancer Genet Cytogenet.* 1993;65(1):51-7.
- West RR, Stafford DA, White AD, Bowen DT, Padua RA. Cytogenetic abnormalities in the myelodysplastic syndromes and occupational or environmental exposure. *Blood* 2000;15;95(6):2093-7
- Mohamedali AM, Gaken J, Twine NA, Ingram W, Westwood N, Lea NC, et al. Prevalence and prognostic significance of allelic imbalance by single-nucleotide polymorphism analysis in low-risk myelodysplastic syndromes. *Blood* 2007;110:3365-73.
- Gaymes TJ, Mufti GJ, Rassool FV. The Non Homologous End-Joining Pathway is Aberrant in Human Myeloid Leukemias: Evidence that KU70/86 is required for the Increased Frequency of Misrepair. *Canc Res.* 2002;62:2791-7.
- Gaymes TJ, Shall S, Macpherson LJ, Twine NA, Lea NC, Farzaneh F, et al. Inhibitors of poly (ADP-ribose) polymerase (PARP) selectively induce apoptosis of myeloid leukemic cells: potential for therapy of acute myeloid leukemia and myelodysplastic

- tic syndromes. *Haematologica* 2009; 94(5):638-46.
10. Bunting SF, Callén E, Wong N, Chen HT, Polato F, Gunn A, et al. 53BP1 inhibits homologous recombination in Brca1-deficient cells by blocking resection of DNA breaks. *Cell*. 2010;14:243-54.
  11. Haince JF, McDonald D, Rodrigue A. PARP1-dependent kinetics of recruitment of MRE11 and NBS1 proteins to multiple DNA damage sites. *J. Biol Chem*. 2008; 283:1197-208.
  12. McCabe N, Turner NC, Lord CJ. Deficiency in the repair of DNA damage by homologous recombination and sensitivity to poly(ADP-ribose) polymerase inhibition. *Cancer Res*. 2006;15:8109-15.
  13. Li HR, Shagisultanova EI, Yamashita K, Piao Z, Perucho M, Malkhosyan SR. Hypersensitivity of tumor cell lines with microsatellite instability to DNA double strand break producing chemotherapeutic agent bleomycin. *Cancer Res*. 2004;15: 4760-7.
  14. Diouf B, Cheng Q, Krynetskaia NE. Somatic deletions of genes regulating MSH2 protein stability cause DNA mismatch repair deficiency and drug resistance in human leukaemia cells. *Nat Med*. 2011;17:1298-303.
  15. Suraweera N, Duval A, Reperant M. Evaluation of tumor microsatellite instability using five quasimonomorphic mononucleotide repeats and pentaplex PCR. *Gastroenterology* 2002;123:1804-11.
  16. Sutter C, Gebert J, Bischoff P, Herfarth C, von Knebel Doeberitz M. Molecular screening of potential HNPCC patients using a multiplex microsatellite PCR system. *Mol Cell Probes* 1999;13:157-65.
  17. Hoang JM, Cottu PH, Thuille B, Salmon RJ, Thomas G, Hamelin R. BAT-26, an indicator of the replication error phenotype in colorectal cancers and cell lines. *Cancer Res*. 1997;57:300-3.
  18. Wen Q, Scorah J, Phear G, Rodgers G, Rodgers S, Meuth M. A mutant allele of MRE11 found in mismatch repair-deficient tumor cells suppresses the cellular response to DNA replication fork stress in a dominant negative manner. *Mol. Biol. Cell* 2008; 19:1693-705.
  19. Pawlik TM, Raut CP, Rodriguez-Bigas MA. Colorectal carcinogenesis: MSI-H versus MSI-L. *Dis. Markers*. 2004;20:199-206.
  20. Laiho P, Launonen V, Lahermo P, Esteller M, Guo M, Herman JG, et al. Low-level microsatellite instability in most colorectal carcinomas. *Cancer Res*. 2002;15(62):1166-70
  21. Halford SE, Sawyer EJ, Lambros MB, Gorman P, Macdonald ND, Talbot IC, Foulkes, et al. MSI-low, a real phenomenon which varies in frequency among cancer types. *J Pathol*. 2003;20:389-94.
  22. Sill H, Goldman JM, Cross NC. Rarity of microsatellite alterations in acute myeloid leukaemia. *Br J Cancer*. 1996;74:255-7.
  23. Casorelli I, Offman J, Mele L, Pagano L, Sica S, D'Errico M, et al. Drug treatment in the development of mismatch repair defective acute leukemia and myelodysplastic syndrome. *DNA Repair*. 2003;2:547-59.
  24. Kambara T, Matsubara N, Nakagawa H, Notohara K, Nagasaka T, Yoshino T, et al. High frequency of low-level microsatellite instability in early colorectal cancer. *Cancer Res*. 2001;1:7743-6.
  25. Ludwig L, Schulz AS, Janssen JW, Grünewald K, Bartram CR. P53 mutations in myelodysplastic syndromes. *Leukemia*. 1992;6(12):1302-4
  26. Fordham SE, Matheson EC, Scott K, Irving JA, Allan JM. DNA mismatch repair status affects cellular response to Ara-C and other anti-leukemic nucleoside analogs. *Leukemia* 2011;25:1046-9.
  27. Allan JM, Travis LB. Mechanisms of therapy-related carcinogenesis. *Nat Rev Cancer* 2005; 5:943-55.
  28. Karran P, Offman J, Bignami M. Human mismatch repair, drug-induced DNA damage, and secondary cancer. *Biochimie* 2003;85:1149-60.
  29. Giannini G, Rinaldi C, Ristori E, Ambrosini MI, Cerignoli F, Viel A, et al. Mutations of an intronic repeat induce impaired MRE11 expression in primary human cancer with microsatellite instability. *Oncogene*. 2004; 23:2640-7.
  30. Ejima Y, Yang L, Sasaki MS. Aberrant splicing of the ATM gene associated with shortening of the intronic mononucleotide tract in human colon tumor cell lines: a novel mutation target of microsatellite instability. *Int J Cancer*. 2000;86:262-8.
  31. Takeda S, Nakamura K, Taniguchi Y, Paull TT. Ctp1/CtIP and the MRN complex collaborate in the initial steps of homologous recombination. *Mol. Cell* 2007;9:351-2.
  32. Grenon M, Gilbert C, Lowndes NE. Checkpoint activation in response to double-strand breaks requires the MRE11/Rad50/Xrs2 complex. *Nat Cell Biol*. 2001;3:844-7.
  33. Trenz K, Smith E, Smith S, Costanzo V. ATM and ATR promote MRE11 dependent restart of collapsed replication forks and prevent accumulation of DNA breaks. *EMBO J*. 2006;25:1764-74.
  34. Yu X, Wu LC, Bowcock AM, Aronheim A, Baer R. The C-terminal (BRCT) domains of BRCA1 interact in vivo with CtIP, a protein implicated in the CtBP pathway of transcriptional repression. *J. Biol. Chem*. 1998; 273:25388-92.
  35. Chen PL, Liu F, Cai S, Li A, Chen Y, Gu B, et al. Inactivation of CtIP leads to early embryonic lethality mediated by G1 restraint and to tumorigenesis by haploid insufficiency. *Mol. Cell. Biol*. 2005;25:3535-42.
  36. Meloni AR, Smith EJ, Nevins JR. A mechanism for Rb/p130-mediated transcription repression involving recruitment of the CtBP corepressor. *Proc Natl Acad Sci USA*. 1999;96:9574-9.
  37. Chakraverty RK, Hickson ID. Defending genome integrity during DNA replication: a proposed role for RecQ family helicases. *Bioessays* 1999;21:286-94.